Environmental Microbiome

RESEARCH Open Access

Diversity and functional features of the root-associated bacteriome are dependent on grapevine susceptibility to *Plasmopara viticola*

Morgane Duret[1†], Adrian Wallner[1†], Ludovic Besaury[2] and Aziz Aziz[1*]

Abstract

Background Plant health depends on beneficial interactions between the roots and their microbiomes. Despite recent progress on the role of the grapevine microbiome, the taxonomic identity and functional traits of microbial taxa specific to healthy or *Plasmopara viticola*-diseased plants, as well as to the susceptible or resistant cultivar are unknown. Using metabarcoding and shotgun metagenomics sequencing, we investigated the effect of downy mildew on the root-associated microbiome (rhizospheric soil, rhizoplane and endosphere) of 41B-grafted susceptible cultivar (Chardonnay) and resistant interspecific hybrid (Voltis) at flowering and veraison stages. The impact of conventional treatment on the rhizomicrobiome assembly of Chardonnay was also evaluated.

Results Analyses revealed a core bacteriome shared between both susceptible and resistant cultivars. This also highlighted common functional traits between the rhizosphere and rhizoplane bacteriomes in both cultivars. A dysbiosis state was also evidenced by a loss of beneficial communities in the rhizosphere of the *P. viticola*-infected cultivar. Microbial genome assemblies showed functional differences between healthy and diseased plants, with a loss of *Pseudomonas* and *Phyllobacterium* taxa at veraison. This state was mainly characterized by a loss of genes involved in polyamine transport and metabolism in the susceptible cultivar. It was also marked by an increase in population evenness and total bacterial diversity, and the presence of pathogenic species in susceptible plants.

Conclusions This study reveals distinct and overlapping bacterial communities and functional genes in the rhizospheric soil, rhizoplane and root endosphere of both susceptible and resistant grapevine cultivars to downy mildew. Microbial diversity and abundant taxa of grapevine roots are influenced by downy mildew and cultivar susceptibility. Common bacterial functions are shared among rhizocompartments of susceptible and resistant cultivars, revealing a dysbiosis state and functional signatures related to plant immunity, especially in the infected-susceptible plants.

†Morgane Duret and Adrian Wallner contributed equally to this study.

*Correspondence:
Aziz Aziz
aziz.aziz@univ-reims.fr

Full list of author information is available at the end of the article

Keywords Cultivar, Disease resistance, Functional features, Grapevine, Microbiome, *Plasmopara viticola*, Root-associated microbiota

Background

Plants live in association with a wide range and complex assembly of microbes including bacteria, archaea, oomycetes, fungi and protists [1]. These microbial assemblages, collectively referred to as the plant microbiota, can be considered as a part of their extended phenotype and as such, play a major role in various steps of the plant's life cycle [2, 3]. The assembly of the rhizosphere microbiome is mainly determined by the chemistry surrounding plant roots, including root exudates and cell wall components. The contribution of the soil and root microbiomes to plant growth and health promotion is a trait of particular interest in the quest for sustainable agriculture practices. Across plant species and cultivars, both rhizospheric and endophytic microbes repeatedly exhibited the capacity to influence their host's resilience to biotic and abiotic stresses [4–7]. Recent studies provide new insights into the colonization of plant roots by specific microbial taxa and the systemic response associated with improved plant health and performance under a variety of biotic and abiotic stresses [8]. These beneficial microbes can directly antagonize pathogenic microbes or prime plants for enhanced local and systemic immunity through hormonal signaling pathways [9, 10]. The microbial assembly is influenced by multiple factors, including plant genotypes, agricultural practices, or seasonality, impacting the taxa and functions retrieved in the plant microbiomes [11, 12]. The aboveground parts of plants can also influence the structure and function of the rhizosphere and root-associated microbiomes through the modulation of root metabolism upon perception of specific pathogens [13]. Thus, sustainably engineering the root associated microbial communities could represent a cost-effective and eco-friendly alternative to pesticide treatments.

Grapevine (*Vitis vinifera* L.) has become the most economically important fruit species in the world, due to the many uses of its fruit for the production of table grapes, dried fruit, juice, wine and organic compounds of therapeutic and cosmetic interest [14]. However, recurrent diseases caused by destructive pathogens such as *Plasmopara viticola*, responsible for downy mildew, become a huge threat to the sustainability of grape production [15]. The control of these diseases is generally achieved by widespread applications of chemical fungicides, which become major concerns for human health and the environment [15]. As alternative, several diseases resistant cultivars were generated through breeding programs, including Voltis which possesses resistance genes against *P. viticola* (*Rpv1/Rpv3*) and *Erysiphe necator* (*Run1/Ren3*) [16]. However, adopting such mildew-resistant hybrids is still uncertain in terms of their level of tolerance to other diseases and their performance under various conditions.

Improving functional microbial diversity is among the most promising and innovative levers in vineyard systems, since grapevine is naturally colonized by a wide variety of both prokaryotic and eukaryotic microbes, which may play a great role in fruit yield and grape quality [17]. Some soil beneficial microbes, or microbial consortia are recognized to act as natural biological control agents, thanks to their ability to enhance plant immunity and to their antagonism towards grapevine pathogens [18–21]. Nevertheless, the root-associated microbial communities are rarely investigated in disease contexts in vineyards. When affected by Pierce's disease, a higher sap microbial diversity was observed under moderate symptoms, compared to low or severe symptoms [22]. The survey of plants symptomatic and asymptomatic plants affected by grapevine trunk diseases (GTD) revealed co-occurrence and exclusion patterns which could lead to the identification of GTD-promoting and GTD-suppressing microbes. For instance, a co-occurrence of *Acremonium* sp., a non-GTD related fungus, with the fungi usually associated to GTD in symptomatic grapevines was highlighted, while asymptomatic plants were enriched with specific rhizobacteria, such as *Bacillus* and *Streptomyces*, suggesting their potential contribution to control GTD [23]. These results could support the concept of dysbiosis state, or cry-for-help strategy [24, 25].

While a recent study investigated the impact of downy mildew on the grapevine leaf microbiome, the repercussions of this disease at the whole plant scale is still unknown [26]. Other studies showed that the vine's phyllospheric microbial communities are driven by plant genetic diversity [27, 28], but also by geographic location often called "terroir" [29, 30] and growing season [31]. Chemical treatments seem to exert only minor effects on the richness and diversity of non-targeted bacterial and fungal communities [31, 32]. However, the impact of specific diseases and chemical treatments on the root-associated microbiome is not yet elucidated in grapevine cultivars with contrasting susceptibility to downy mildew.

In this study, we aimed to investigate the richness and diversity of microbial communities associated with grapevine roots under disease pressure in order to identify microbial signatures and their functional role in plant health. To this end, we used metabarcoding and shotgun metagenomics sequencing to examine the root-associated microbiomes of two grapevine cultivars differing in their susceptibility to downy mildew. Experiments were

conducted in the same vineyard that has never been treated with chemicals, and microbial analyses were performed on rhizocompartments (rhizosphere, rhizoplane and endosphere) of susceptible (Chardonnay) and resistant (Voltis) cultivars at full flowering (before the onset of disease) and veraison (after disease expression). The susceptible cultivar, Chardonnay, showed severe symptoms at the veraison stage, while the resistant cultivar Voltis showed very low symptoms. The effect of conventional treatment was also evaluated on the microbiome assembly in the susceptible cultivar to understand the relationship between shoot treatment and the steady state of root-associated microbial diversity.

Methods

Vineyards, root and rhizosphere soil samplings

Experiments were carried out on two grapevine (*Vitis vinifera* L.) cultivars differing in their susceptibility to downy mildew (*P. viticola*), grown in the same vineyards of the Champagne Committee in Chouilly, France. Roots and rhizospheric soil were collected from both susceptible, Chardonnay (clone 121) and resistant, Voltis (clone 1266), grafted on the same rootstock 41B and grown in a vineyard that has never been treated with chemicals. Additional samples were also taken from another plot of Chardonnay plants grown under conventional treatment. Three samples of young roots (≤ 2 mm diameter) and rhizospheric soil were collected from three different plants of each cultivar and condition, at full flowering and veraison stages. Samples were collected using ethanol sterilized transplanting shovel and pruning shears from a depth of approximately 20 cm and within 30 cm of the trunk. No symptoms were identified in both cultivars at flowering, while at the veraison stage, the untreated susceptible cultivar Chardonnay showed a heavy mildew infection (Supplementary Fig. S1). The resistant cultivar Voltis and the chemical-treated Chardonnay displayed strong protection against downy mildew disease. Roots and rhizospheric soil were transferred into clean bags closed hermetically, stored on ice and transported back to the laboratory where they were immediately fractionated.

The rhizospheric soil, rhizoplane and endosphere fractions were separated following the protocol of Edwards et al. [33] with small modifications and stored in sterile Phosphate Buffered Saline (PBS) pH 7.4 buffer at -80 °C. For each sample, 2 g of roots with adhering soil were separated and washed in 20 mL PBS solution by shaking for 15 s with a vortex. The washed roots were then removed for downstream procedures and the remaining medium was stored as the rhizospheric soil fraction. The roots were washed three more times in 20 mL of fresh PBS by shaking them 15 s and changing the washing buffer between each repetition. The washed roots were then sonicated at 45 kHz for 30 s using an ice water bath. The resulting liquid fraction was stored as the rhizoplane fraction and the roots were transferred to 20 mL of fresh PBS for three additional sonication steps of 30 s at 45 kHz with fresh washing buffer at each step. The unsterilized sonicated roots were crushed at room temperature in 2 mL PBS per 0.5 g of roots using sterile mortar and pestle. The final lysate was stored as the endosphere fraction.

DNA extraction and high-throughput sequencing

Total DNA was extracted from the three separated root fractions of each sample. Rhizospheric soil and rhizoplane samples, prepared as described above, were centrifuged at 15,000 g and the supernatant discarded. Depending on the sample, up to 200 mg from the rhizospheric soil and 17 mg from the rhizoplane fractions were used as input material for DNA extraction using the DNeasy PowerSoil Pro Kit (Qiagen) following the manufacturer's instructions. For the endosphere fraction, stored root lysate was centrifuged at 16,000 g for 1 min and up to 50 mg of the pellet were used as input material for DNA extraction using the DNeasy Plant Pro Kit (Qiagen) following the manufacturer's instructions with some modifications. The endosphere fraction was extracted considering the high level of phenolic compounds in grapevine roots, and 400 µL of CD1 and 100 µL of PS were added accordingly at the first extraction step. Five additional membrane washing steps were applied before using the AW1 buffer with 600 µL of 5.5 M guanidium thiocyanate to increase final DNA quality.

Total DNA from all three fractions was further processed by Genoscreen (Lille, France) for the shotgun metagenomic sequencing and by Macrogen (Seoul, South Korea) for the metabarcoding analysis. Shotgun metagenomic sequencing libraries were prepared using the Illumina DNA Prep kit and processed using a 2×150 bp paired-end approach on an Illumina MiSeq with a sequencing depth of 2×10^7 paired-end reads per sample. Metabarcoding libraries were prepared using the Herculase II Fusion DNA Polymerase Nextera XT Index V2 Kit targeting the V3-V4 regions of bacterial 16S rRNA with primers 337F (5'-GACTCCTACGGGAGGCWGCAG-3') and 800R (5'-TACCAGGGTATCTAATCC-3') following manufacturer's instructions [34]. Blank samples, resulting from a buffer extraction, were produced for each type of extraction kit and included in each sequencing procedure.

Processing of Illumina sequence data for functional and taxonomic identification

For shotgun metagenomic sequencing results, paired-end reads were filtered, trimmed and joined using Fastp v0.23.2 [35] retaining only reads longer than 90 nucleotides after trimming based on a quality score of Q25. Reads presenting more than two occurrences of

uncertain bases were discarded. Base corrections of overlapping sequences and over-representation analyses were enabled. Paired-end read joining was performed with a minimal overlap of 30 bases. Only merged reads were retained for downstream procedures. Reads were mapped separately to the mgPGPT vFeb2022 database from PLaBAse [36] and to the AnnoTree vJune2021 database [37, 38] using the Diamond v2.0.9 sequence alignment tool, with an e-value cutoff at 1×10^{-10} for the blastx function [39]. In addition to the functional affiliation, taxonomic classification was performed using the NCBI non-redundant protein sequences database v2022-03-10 with Kaiju v1.9.0 [40]. Filtered and trimmed reads were further used for assembly using Megahit v1.2.9 on paired-end libraries with the recommended settings for complex metagenomes [41]. To improve de Bruijn graph building efficiency, six library groups were used separately for genomic assemblies according to the plant cultivar and sampling season. For each of the six sample groups, the 50 longest assemblies were used for taxonomic prediction using BlastN against NCBI's nucleotide database [42].

Metagenome-assembled genomes

The metagenome assembled genomes (MAGs) were analyzed for completeness and contamination levels with checkM v1.2.2 [43] and their taxonomic affiliation predicted with GTDB-Tk v2.1.1 [44]. Sixteen MAGs with medium to high quality (>60% completeness and <15% contamination) were further annotated using the MicroScope platform [45]. The whole genomes were classified into different orthologous groups and annotated using the EGGNOG (v5.0.2). The differentially abundant bacterial biomarker identified with LEfSe (v2.31) in shotgun metagenomic results and associated with plant-beneficial functions were targeted in MAGs. For this purpose, the names associated to the KEGG functions were searched on any computational results obtained with the MicroScope pipeline using keywords research. The functions were considered as retrieved only when the "Product" column was corresponding to the identified KEGG function in metagenomic analyses.

16 S rRNA sequencing and metabarcoding

The 16 S rRNA sequencing and metabarcoding raw reads were evaluated for their read qualities using Qiime2 v2022.8 [46]. Primer sequences were first trimmed using Cutadapt [47]. Paired-end reads were further filtered and joined using DADA2 [48]. Individual reads were truncated at the first occurrence of a base below a quality level of Q20 and discarded when containing more than two expected errors. After read joining, chimeric sequences were removed using the consensus method. Taxonomic classification for all ASVs was obtained with a Naive Bayes classifier [49] trained on the Silva v138.1 database collapsed at 99% sequence identity [50]. Phylogenetic trees used to examine beta-diversity were generated by sequence alignment using MAFFT [51], which was then processed using FastTree [52]. The sequencing outputs from control samples were used for decontamination of the remaining dataset using the decontam v1.12 package [53] using the prevalence method at a threshold level of 0.1.

Statistical analysis

Downstream diversity and statistical analyses were performed using phyloseq v1.38.0 [54]. Statistic comparisons between alpha-diversity values were obtained through ANOVA tests and refined through the Tukey HSD analysis. For beta-diversity metrics, a PERMANOVA method was used. Differential abundant bacterial biomarkers were identified using LEfSe v2.31 [55]. When analyzing the effect of plant cultivar and chemical treatment, the root fractions are used as a subclass to improve the robustness of predicted biomarkers. A per-sample normalization of the sum of the values to 1 M reads was applied and a 0.05 *p*-value cutoff used for the Kruskal-Wallis and Wilcoxon tests prior to the linear discriminant analysis. Core components of microbial populations were estimated by considering a combination of the three root compartments for each plant cultivar and phenological stage.

Results

Amplicon sequencing and shotgun metagenomics of grapevine root-associated microbiota

The amplicon sequencing and shotgun metagenomics analyses were carried out on the rhizospheric soil, rhizoplane and endosphere of 41B-grafted Chardonnay (susceptible cultivar) and Voltis (resistant interspecific hybrid) at flowering and veraison stages from a same vineyard that has never been treated with chemicals. Analyses were also performed on chemical treated-Chardonnay from a separate plot (hereafter treated Chardonnay). All sampled plants were asymptomatic at flowering. At veraison, Voltis remained largely asymptomatic, the treated Chardonnay showed few symptoms of downy mildew, while the untreated Chardonnay was heavily diseased (Supplementary Fig. S1). After quality control, 3,674,254 16 S paired-end sequences were obtained from 57 samples and a total of 52,429 ASVs were identified. Rarefaction curves for bacterial ASVs attest of a good sequencing depth enabling robust analyses of community compositions (Supplementary Fig. S2).

Shotgun metagenomics were performed only on rhizoplane and rhizospheric soil samples to avoid excessive contamination from plant DNA. Overall, 931,971,864 paired-end sequences were obtained from 37 samples

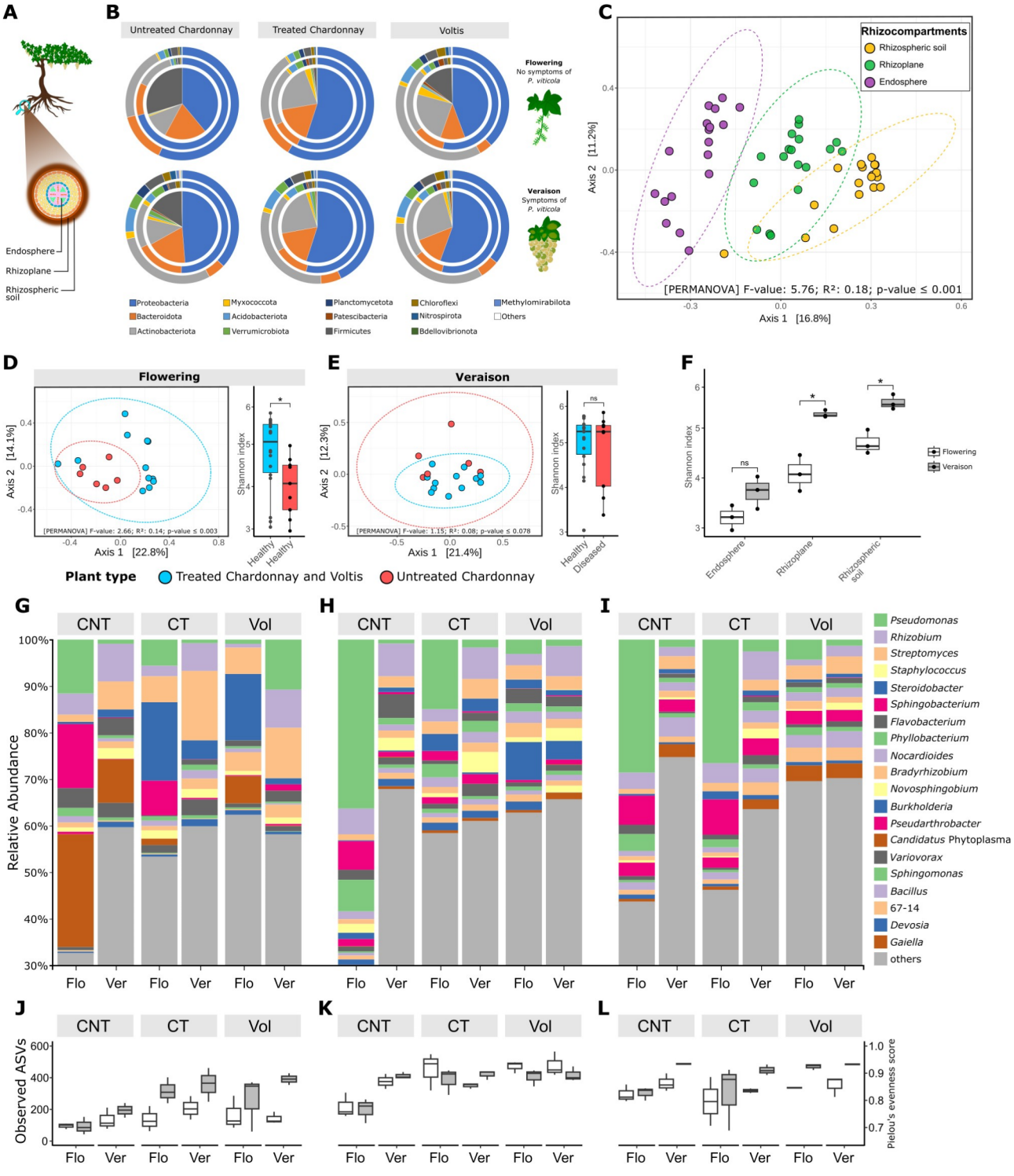

Fig. 1 (See legend on next page.)

with 91.32% of sequences > Q30. Raw sequence processing resulted in a total of 107,249,181 final sequences for downstream analyzes. Blank samples subjected to shotgun metagenomics were not biased by the amplification step of metabarcoding and provide a truthful overlook of the kit contamination. For all extraction kits, these blank samples presented a low number of reads (0.0019% of the mean experimental sample) with 34% of predicted duplicate reads.

(See figure on previous page.)

Fig. 1 Taxonomical composition, beta-diversity of bacterial communities and relative abundance of bacterial genera in the endosphere, rhizoplane and rhizospheric soil of susceptible and resistant cultivars. **A**: Representation of a grapevine root cross-section depicting the delimitation between the endosphere, rhizoplane and rhizospheric soil. **B**: Taxonomical composition of bacterial communities in the rhizocompartments of Chardonnay (untreated and treated) and Voltis, at flowering (absence of *P. viticola*), and veraison (presence of *P. viticola*). For each condition, the microbial communities are represented on the root cross-section, with central pie-chart for the endosphere, and external pie-charts for the rhizoplane and the rhizospheric soil. The top 13 taxa were shown. **C**: Beta-diversity of bacterial communities in rhizocompartments of susceptible (treated and untreated) and resistant cultivars. Beta diversity was calculated using Bray-Curtis distance and statistically tested by the PERMANOVA test. The beta-diversity was visualized by the principal coordinate analysis (PCoA) plots for bacterial communities. **D**, **E**: Beta-diversity of bacterial communities from the rhizoplane and rhizospheric soil of healthy Voltis, treated Chardonnay and untreated Chardonnay plants at flowering (before downy mildew infection) (**D**) and at veraison (after downy mildew infection) (**E**). Beta-diversity was calculated using Bray-Curtis distance and statistically tested by the PERMANOVA test. The beta-diversity was visualized by the principal coordinate analysis (PCoA) plots for bacterial communities. The alpha-diversity levels between healthy (treated Chardonnay and Voltis) and diseased (untreated Chardonnay) plants were compared using Shannon index. Significance levels were obtained through Wilcoxon test (*, $p \leq 0.05$; ns, not significant). **F**: Comparison of alpha-diversity levels between the root fractions of untreated Chardonnay at flowering and veraison. Significance levels were obtained through a Wilcoxon test (* = $p \leq 0.05$; ns = not significant). **G**, **H**, **I**, **J**, **K**, **L**: Relative abundance of bacterial genera obtained by metabarcoding analysis of the endosphere (**G**), rhizoplane (**H**) and rhizospheric soil (**I**) of susceptible and resistant cultivars. Data show the top 20 taxa, and other minors grouped together, from untreated Chardonnay (CNT), treated Chardonnay (CT) and Voltis (Vol) at flowering (Flo) and veraison (Ver). Data are means of three replicates. The corresponding diversity obtained by metabarcoding in the endosphere (**J**), rhizoplane (**K**) and rhizospheric soil (**L**) was measured as number of observed ASVs (white) and Pielou's evenness index (grey). Data are means of three replicates

Amplicon sequencing results were used to get an overview of the bacterial composition in Voltis and Chardonnay root fractions at flowering and veraison, and in response to fungicide treatments (Fig. 1A-B, Supplementary Table S1). Data showed that microbiome compositions varied with rhizocompartments, cultivars and treatment. Across all samples, reads were primarily classified as Proteobacteria (50.32% of assigned reads), Actinobacteria (22.61%), Bacteroidota (11.93%), Firmicutes (5.13%), Acidobacteriota (2.70%), Verrumicrobiota (2.13%), Myxococcota (1.42%), Planctomycetota (1.16%), Chloroflexi (1.04%), Patescibacteria (0.54%), Nitrospirota (0.42%), Methylomirabilota (0.19%), Bdellovibrionota (0.10%), Gemmatimonadota (0.10%), Latescibacterodota (0.04%), Entotheonellaeota (0.04%), NB1-J (0.03%), and other poorly represented bacteria (0.08%).

The endosphere, rhizoplane and rhizosphere compartments exhibit distinct microbial compositions with some differences between flowering and veraison (Fig. 1A, Supplementary Table S1). Among the most abundant taxa, Proteobacteria are abundant in all plants. Actinobacteria are more abundant in the rhizosphere compared to the rhizoplane and endosphere in Voltis and untreated Chardonnay at both stages, as well as in treated Chardonnay at veraison. Bacteroidota are more abundant in the endosphere of all plants, while Firmicutes are particularly abundant in the endosphere of untreated Chardonnay at both stages, and in the endosphere of Voltis at flowering. Acidobacteriota are more abundant in the rhizosphere and show a decreasing gradient from the rhizosphere to the endosphere, except in treated Chardonnay at flowering. However, Patescibacteria are less abundant in the rhizosphere of all plants, whereas the Methylomirabilota are more abundant in this compartment than others. Overall, marked differences in bacterial communities are observed between the endosphere and rhizosphere, while the rhizoplane shows some similarities with either compartment in terms of proportion. When combining all rhizocompartments, untreated Chardonnay presents more Proteobacteria and Bacteroidota, and less Actinobacteria than Voltis at flowering. At veraison, a reduction of the proportion of Proteobacteria and Bacteroidota, and an increase in Actinobacteria were observed for untreated Chardonnay. An opposite trend was observed for Voltis at veraison. In both cultivars we observed an increase in the proportion of less abundant taxa at veraison (Chloroflexi, Nitrospirota, Gemmatimonadota, NB1-j, Entotheonellaeota, Latescibacterota…), the increase being more marked in untreated Chardonnay and in the rhizosphere compared to the other rhizocompartments. The remaining minor taxa represent about 0.01–0.19% for Chardonnay, and 0.07 to 0.04% for Voltis. Both treated and untreated Chardonnay share overlapping microbial composition marked by a reduction of Proteobacteria and Bacteroidota and an increase of Actinobacteriota at veraison. However, an enrichment in Myxococcota and Patescibacteria, and a loss of Firmicutes is observed in untreated Chardonnay, while the opposite was observed in treated Chardonnay.

Microbial diversity of grapevine roots is influenced by downy mildew

Considering all variables that could be involved in shaping bacterial communities in the analyzed samples, only the rhizocompartment led to significant community clustering (Fig. 1C). To refine community comparisons, the samples were pooled to collapse several variables. We grouped the rhizoplane and rhizospheric soil communities as they show some convergence compared to endophytic communities. Samples from the resistant hybrid Voltis and chemical-treated Chardonnay, that showed only slight symptoms of downy mildew, were further grouped together, while samples from untreated Chardonnay, which are heavily diseased, were categorized

separately. Using this refined discriminating variables, rhizosphere bacterial communities of untreated Chardonnay plants at flowering are significantly different from those found in Voltis and treated Chardonnay plants (Fig. 1D-E). However, this difference is greatly mitigated at veraison, as the microbial communities of both heavily diseased and non-diseased plant groups become similar.

The susceptible untreated Chardonnay plants exhibit a lower alpha-diversity at flowering stage than the combined resistant cultivar Voltis or the treated Chardonnay (4.00 and 4.78 respectively) (Fig. 1D-E). While the diversity levels of the latter do not evolve at veraison (4.99), communities associated with diseased (untreated) Chardonnay seem to reach the same diversity score as the non-diseased plants (Voltis and treated Chardonnay) (4.84). This increase in alpha-diversity was consistent for all rhizocompartments of diseased Chardonnay (from 3.21 to 3.72 for the endosphere, 4.09 to 5.28 for the rhizoplane and 4.70 to 5.51 for the rhizosphere) (Fig. 1F).

Abundant rhizospheric microbial taxa are affected by the cultivar's susceptibility to disease

The relative abundance of bacterial populations associated with roots of untreated Chardonnay is significantly different when comparing the most abundant taxa at the genus level at flowering and veraison. In the endosphere and rhizoplane, 20 genera represent close to 70% of the bacterial diversity at flowering and their representativity falls below 40% at veraison (Fig. 1G-H, J-K). The same difference is observed in the rhizospheric soil (Fig. 1I-L). The large proportions of enriched taxa in the susceptible cultivar at flowering are *Pseudomonas* in the rhizosphere (29.75%) and in the rhizoplane (39.04%), and *Candidatus* Phytoplasma (29.80%) in the endosphere, followed by *Pseudomonas* (13.65%). At veraison, the most enriched taxa are *Bacillus* (4.08%), *Allorhizobium-Neorhizobium-Pararhizobium-Rhizobium* (4.52%), and *Candidatus* Phytoplasma (15.62%), in the rhizosphere, rhizoplane and endosphere respectively. However, the resistant cultivar Voltis displays a high stability amongst its most abundant bacterial taxa between flowering and veraison, particularly in the rhizoplane and rhizosphere compartments, each representing less than 10% of the total taxa (Fig. 1H-I). In the endosphere of Voltis, the most abundant genera at flowering are *Candidatus* Phytoplasma (13.98%), *Steroidobacter* (8.96%), *Bradyrhizobium* (5.38%) and *Streptomyces* (5.29%%). However, the most endosphere-abundant taxa at veraison are *Streptomyces* (13.56%), *Acinetobacter* (7.50%), *Pseudomonas* (7.37%) and *Allorhizobium-Neorhizobium-Pararhizobium-Rhizobium* (5.67%).

The distinct states of the microbial abundance between susceptible and resistant cultivars may reflect initial differences in community assembly. The most abundant taxa for treated Chardonnay are *Pseudomonas* in the rhizosphere (26.88%) and rhizoplane (15.20%), and *Steroidobacter* (15.80%) in the endosphere at flowering. At veraison, they are *Allorhizobium-Neorhizobium-Pararhizobium-Rhizobium* in the rhizosphere (6.17%) and rhizoplane (6.85%), and *Streptomyces* (13.58%) in the endosphere. In the rhizosphere, the 20 most abundant taxa represent almost 70% of the overall taxa abundance at flowering, while it drops at around 40% at veraison, thus being close to what have been observed in untreated Chardonnay. For the rhizoplane, it went from around 50–40%, which is closest to the Voltis composition. For some genera, their evolution from flowering to veraison were closest to the composition in untreated Chardonnay i.e., less *Sphingobacterium* and *Pseudomonas* in all rhizocompartments, or in Voltis i.e., less *Steroidobacter* in the endosphere and rhizoplane. Differences are also observed at the ASV level (Fig. 1J-L). Importantly, the increased ASVs in both cultivars at veraison is associated with healthy plants (treated Chardonnay and Voltis), and an increase of the bacterial communities' evenness. However, the rhizocompartments of susceptible plants (untreated Chardonnay) at veraison are marked by a reduction of the relative abundance of *Pseudomonas*, *Sphingobacterium* and *Phyllobacterium* communities.

When comparing the differential abundance levels of bacterial genera at flowering, most significant differences were found between the rhizocompartments of the susceptible Chardonnay cultivar and Voltis (Fig. 2A, Supplementary Fig. S3). A total of 42 and 17 genera were enriched in the rhizosphere of Voltis and untreated Chardonnay, respectively, with an LDA score ≥ 2.0. *Kineosporia* was the only resistant cultivar-enriched genus at flowering, but not detected in the susceptible plants. However, the *Enterobacter* and *Niabella* are among the genera that are significantly enriched in the susceptible cultivar at flowering and veraison, respectively, but not detected in Voltis samples. This communities could be linked to the outbreak of downy mildew disease during the veraison phase.

Significant enrichments with an LDA score ≥ 2.0 are also observed by comparing bacterial communities of treated and untreated Chardonnay (Supplementary Fig. S3). The untreated plants were the only ones harboring *Paenibacillus* at both flowering and veraison, whereas *Cryptosporangium* and *D05_2* are only present in treated plants at flowering and veraison, respectively. Moreover, the treated Chardonnay also harbors a low proportion of *Candidatus* Phytoplasma in the endosphere at flowering, and *Enterobacter* in the rhizosphere at veraison. Interestingly, comparison across flowering and veraison of taxonomic composition of untreated Chardonnay highlighted a significant loss of *Pseudomonas*, *Sphingobacterium*, *Phyllobacterium*, *Chryseobacterium*, *Arthrobacter*,

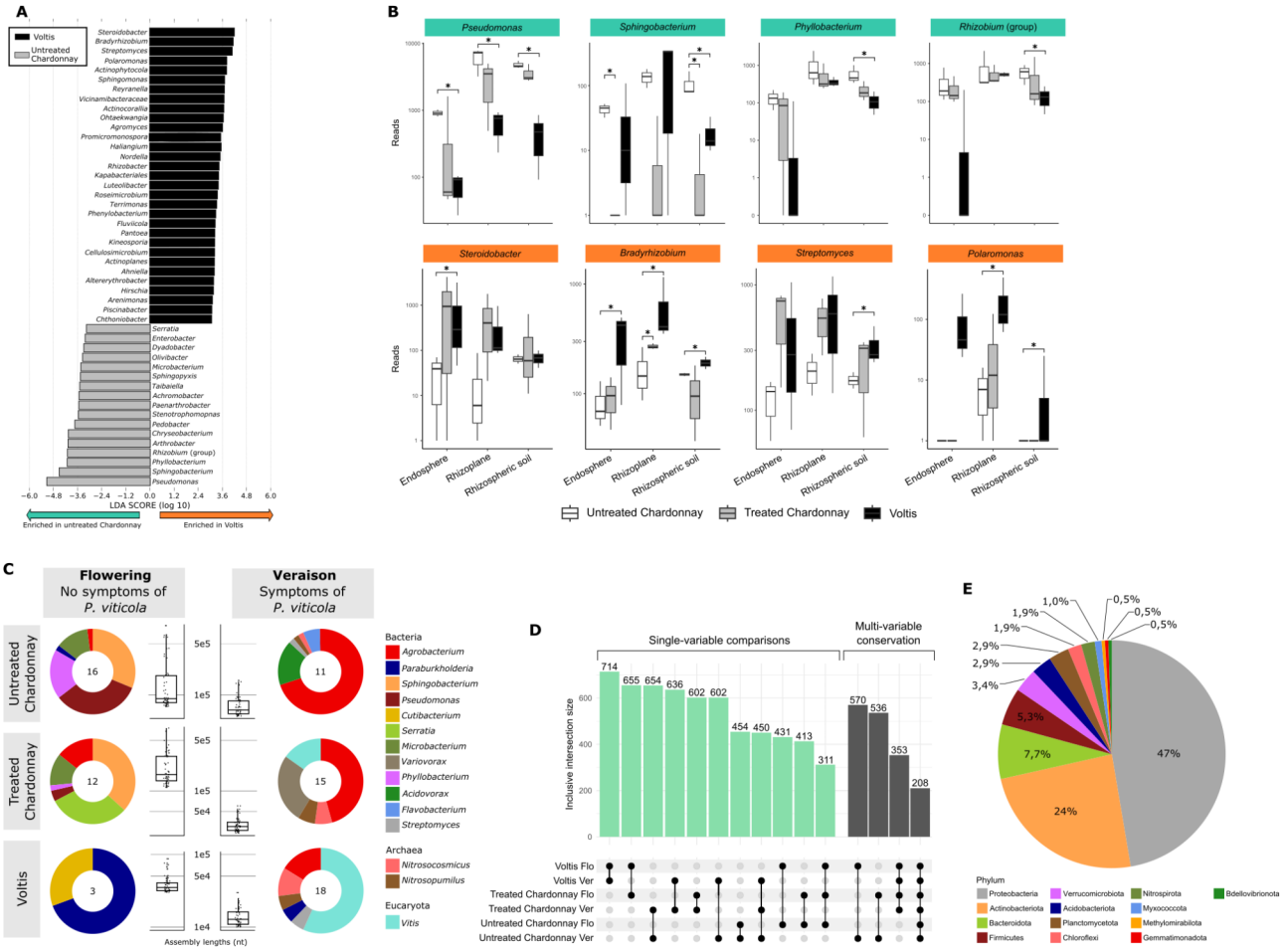

Fig. 2 Colonization patterns of bacterial genera, genome fragment assemblies and core bacterial populations in rhizocompartments of susceptible and resistant cultivars to downy mildew. **A**, **B**: Distinct colonization patterns of bacterial genera between rhizocompartments of grapevine cultivars at flowering. (**A**) Global output of LEfSe analysis between resistant cultivar (Voltis) and susceptible one (untreated Chardonnay), with LDA score ≥ 2.0 cutoff. Taxa with names referring to bacterial clusters were removed from the representation. (**B**) Abundance values for the four most differentially abundant genera between Voltis and Chardonnay. Different letters indicate significant difference using a linear discriminant analysis preceded by pairwise statistical tests (Wilcoxon, *, $p \leq 0.05$; ns, not significant). **C**: Taxonomy and length of the 50 most efficient genome fragment assemblies. Shotgun metagenomic reads were assembled separately for each cultivar and sampling season by pooling the reads from the rhizoplane and rhizospheric soil fractions. The sizes of the 50 longest fragments were determined for each condition and further used for taxonomic prediction and summarized for the overall top 12 most abundant bacterial genera as well as archaea and the grapevine host. The total number of genera represented by the top 50 assemblies is given in the center of the pie charts. Detailed results are shown in supplementary table S2. **D**, **E**: Conserved bacterial populations between samples of untreated Chardonnay, treated Chardonnay and Voltis. (**D**) Conservation of populations at flowering (Flo) and veraison (Ver) at the ASV level considering single variable (green) or multiple variable (grey) differences between samples. The values on the top indicate the number of shared ASVs across the compared conditions. (**E**) Composition of the core bacterial population of 208 ASVs found in all samples at the phylum level

Achromobacter, *Serratia* and *Olivibacter*, and a significant increasing abundance of 32 other genera. Among them, *Olivibacter* was present only at flowering, while *NS11-12_marine_group*, *Blyi10*, *OM190*, *Aquicella*, *P3OB_42*, *LWQ8* and *Acinetobacter* were present only at veraison.

Communities of treated Chardonnay often occupy an intermediate position in terms of abundance and can barely be significantly discriminated from those found in the other plant groups (Fig. 2B, Supplementary Fig. S4). According to the PCA analysis, the treated Chardonnay communities overlap with the untreated Chardonnay and Voltis samples at flowering, regardless of the rhizocompartment (Supplementary Fig. S4). Moreover, the number of reads in treated Chardonnay samples, regarding the most differentially abundant genera, was not significantly different compared to Voltis and untreated Chardonnay at flowering in all compartments. Only *Sphingobacterium* and *Bradyrhizobium* stand out as differentially abundant of other conditions, with less *Sphingobacterium* in the rhizosphere and more *Bradyrhizobium* in the rhizoplane of treated plants compared to the untreated Chardonnay (Fig. 2B).

Metagenomic-supported improvement of taxonomic predictions

Shotgun metagenomic reads and metagenome-assembled genomes (MAGs) were studied to improve community identification in the different samples. Metagenomic reads can lead to more accurate taxonomic predictions as they can detect less conserved markers than the ribosomal RNA sequences targeted by metabarcoding. However, with complex samples like rhizospheric soil, the sequencing depth is not sufficient to achieve diversity saturation and a reliable overview of the total community composition (Supplementary Fig. S5A, B).

Nevertheless, the affiliations of the overall most abundant taxa strongly overlap when using either of the sequencing methods. While metabarcoding identifies the *Pseudomonas* genus as highly abundant (70.10% from all reads) in healthy plants at flowering (Fig. 1G-I), metagenomic analysis shows that *Pseudomonas fluorescens*, *Pseudomonas putida* and *Pseudomonas savastanoi* account for 58.57%, 5.64% and 3.11%, respectively of the genus' prevalence in the rhizosphere and rhizoplane. Further *Pseudomonas* species with lower abundance were also detected e.g., *Pseudomonas entomophilia*, *Pseudomonas coronafaciens*, and *Pseudomonas aeruginosa* (Fig. 1G-I, Supplementary Fig. S5B), with a total of 15 identifies *Pseudomonas* species. The overall second most abundant taxon identified by metabarcoding is the *Allorhizobium-Neorhizobium-Pararhizobium-Rhizobium* group. Metagenomic analysis identified *Agrobacterium tumefaciens* as the second most abundant species, which is genetically close to *Rhizobium*. *Rhizobium leguminosarum*, *Mesorhizobium opportunistum* and *Rhizobium etli* further contribute to the prevalence of the *Rhizobium* group. According to metabarcoding, *Streptomyces* is the third most abundant genus. While no *Streptomyces* species was found in high numbers through metagenomics, this genus is represented by 70 medium-to-low abundance species enriched especially at veraison. Metabarcoding identifies the burkholderia group as the dominating taxon in the rhizoplane of the resistant cultivar Voltis at flowering, and still at strong proportion at veraison. Accordingly, metagenomics predicts *Paraburkholderia phytofirmans* as the main representative of burkholderia in Voltis rhizocompartments.

The MAG approach relies on the assembly of long fragments for increased reliability in taxonomic prediction. For each plant and season, metagenomic reads from the rhizospheric soil, and the rhizoplane were used to generate genome fragment assemblies which were further grouped into MAGs. The 50 longest assemblies of each condition, representing the most abundant organisms, were then used for taxonomic prediction (Fig. 2C, Supplementary Table S2). In the untreated Chardonnay, there is a higher diversity of abundant bacteria at flowering than at veraison. These assemblies allow to identify at flowering *Pseudomonas* (4 species), *Sphingobacterium* (4), *Phyllobacterium* (1), *Microbacterium* (4), *Parabulkholderia* (1) and *Agrobacterium* (1) in the untreated Chardonnay, and *Sphingobacterium* (4), *Serratia* (1), *Agrobacterium* (1), *Microbacterium* (2), *Phyllobacterium* (1) and *Pseudomonas* (1) in the treated Chardonnay. However, in both treated and untreated Chardonnay, the veraison season is characterized by a high abundance of *Agrobacterium* species (4 and 2, respectively), accompanied by *Acidovorax (3)*, *Flavobacterium* (2) and *Streptomyces* (1) in the untreated plants, and *Variovorax* (1) in the treated ones. In Voltis, however, only 3 species including *Paraburkolderia* (1) and *Cutibacterium* (1) were identified at flowering, while at veraison *Agrobacterium* (3), *Paraburkolderia* (1) and *Streptomyces* (1) were identified. Taxa which were classified as low abundant by metabarcoding, such as Archaea or grapevine mitochondria, are only detected using genome fragment assembly of veraison samples (Fig. 2C, Supplementary Table S2). It is striking that the assembly efficiencies are higher in flowering samples, with median fragment lengths 30%, 81% and 65% shorter at veraison for untreated Chardonnay, treated Chardonnay and Voltis, respectively (Fig. 2C). This suggests that the reads at veraison are more evenly distributed among a diversity of microbes, as revealed by the metabarcoding analysis (Fig. 1).

Conservation of bacterial communities between cultivars and growing conditions

To further understand how microbial communities are conserved across plant cultivars and seasons, the ASVs found in the three rhizocompartments were grouped together (Fig. 2D). The most conserved populations are found within and between healthy plants (Voltis and treated Chardonnay) at flowering and veraison. Untreated Chardonnay also shows a strong conservation of bacterial communities with treated Chardonnay and Voltis, but only at veraison. Overall, the resistant cultivar, Voltis has the most conserved community between season with 714 ASVs, followed by treated and untreated Chardonnay with 602 and 454 ASVs, respectively. The increased similarity between the roots of disease-infected and non-infected plants at veraison is confirmed, since the number of conserved bacterial taxa is 30,9% higher than at flowering. Strikingly, bacterial communities of the susceptible plants (untreated Chardonnay) share more ASVs with the healthy plants (Voltis and treated Chardonnay at both stages) at veraison than at flowering.

The overall core-microbiome of Voltis and Chardonnay is composed of 208 bacterial ASVs (Fig. 2E). The core bacterial community is essentially composed of Proteobacteria (47%) and Actinobacteria (24%), and in a smaller

proportion of Bacteroidota (7,7%), Firmicutes (5,3%), Verrumicrobiota (3,4%) and Acidobacteriota (2,9%).

Common bacterial functions are shared among rhizospheric soil and rhizoplane of both susceptible and resistant cultivars

Gene enrichment and functional prediction were achieved through the analysis of shotgun metagenomic sequences. The relevant functions were obtained using the PLant-associated BActeria database (PLaBA-db), a curated list of genes from plant associated bacteria and their KEGG annotation [36].

In both rhizospheric soil and rhizoplane, susceptible cultivar (untreated Chardonnay) and resistant one (Voltis) share common gene enrichments (Fig. 3A). A total of 7 and 15 genes are enriched in the rhizoplane and rhizospheric soil of untreated Chardonnay, respectively, while in Voltis 17 and 22 genes are enriched in these respective fractions. All functions enriched in the rhizoplane of untreated Chardonnay display a conserved enrichment in the equivalent fraction of Voltis, except for the *acrA* gene encoding a membrane fusion protein / multidrug efflux system (K03585). These conserved functions are involved in symbiosis and biofilm formation (*fabG*, K00059; *expr*, K19734; *roeA*, K21022). Similarly, all functions enriched in the rhizospheric soil of untreated Chardonnay are also enriched in Voltis, except for *mdh1* encoding a methanol dehydrogenase (cytochrome c) subunit 1 (K14028). Again, common functions are involved in biofilm production and root colonization (*purB*, K01756; *pilJ*, K02660 and *ubiD*, K03182), as well as DNA recombination, replication and repair with three unclassified putative transposases K07485; K07492; K07493, integrase/recombinase *xerC* (K03733) and dihydropteroate synthase type 2 *sul2* (K18824).

Functional enrichment in the rhizocompartments of treated Chardonnay was limited to the rhizoplane with *ABC.SP.P1* a putative spermidine/putrescine transport system permease protein (K02054).

Root microbiome of susceptible cultivar is enriched in plant-interaction functions

Following the trend observed for the taxonomic community compositions, most functional enrichments were found in untreated Chardonnay at flowering compared to the same plants at veraison or to Voltis at flowering (Fig. 3B). Overall, 14 genes were significantly enriched in the Voltis rhizosphere, whereas 19 genes were more abundant in the untreated Chardonnay rhizosphere at flowering only. Functional groups identified in the

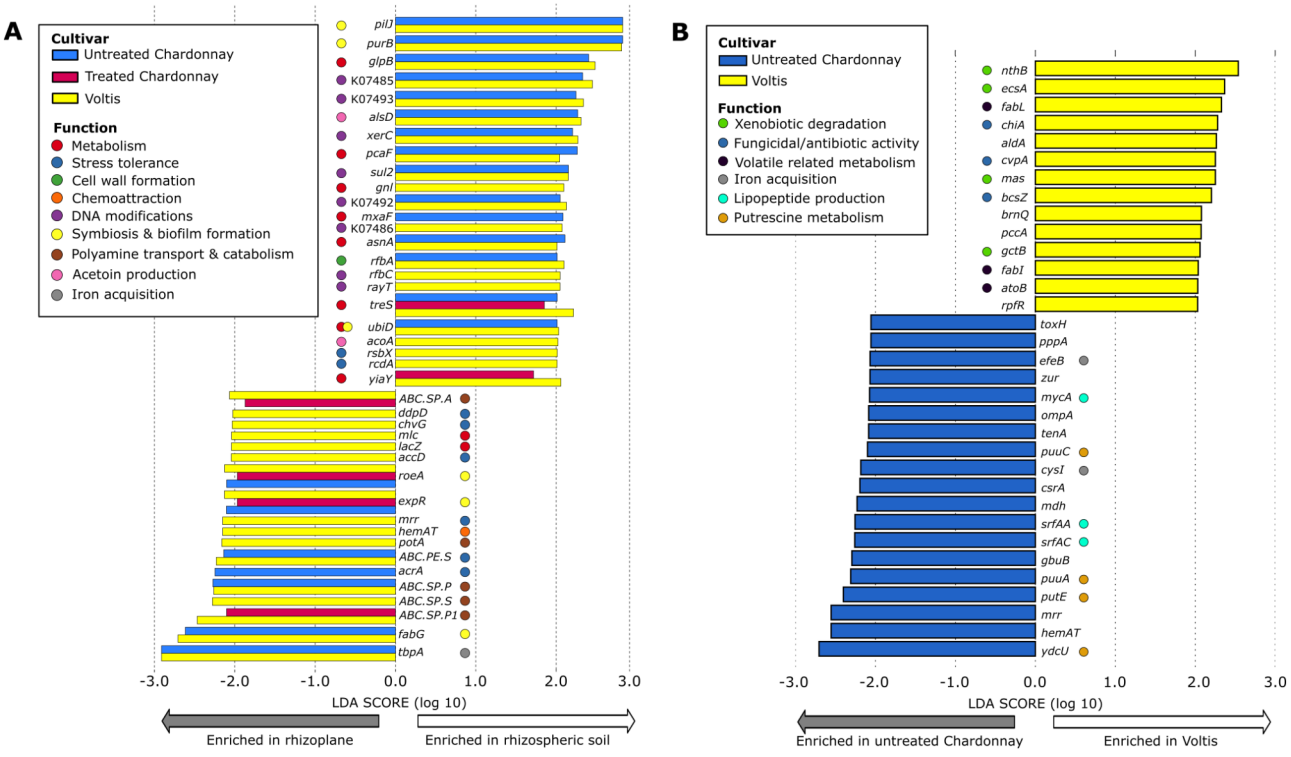

Fig. 3 Differential abundance analysis of bacterial functions in the rhizosphere of susceptible (untreated and treated Chardonnay) and resistant cultivar (Voltis). A linear discrimination analysis was used to infer the differentially enriched bacterial function between rhizospheric soil and rhizoplane of the different conditions (**A**) at flowering and veraison, and between Voltis and untreated Chardonnay at flowering (**B**). In this last case, a focus was made on the functions providing benefits for plants. Prior to building the LDA model, sample size was normalized to 1 × 106, and a 0.05 p-value cutoff was applied for the sequential Kruskal-Wallis and Wilcoxon tests

untreated Chardonnay are related to putrescine transport (*potE*, K03756; *ABC.SP.P1*, K02054) and putrescine degradation (*puuA*, K09470; *kauB*, K12254), iron acquisition (*efeB*, K16301; *cysI*, K00381) and lipopeptide synthesis (*srfAA*, K15654; *srfAC*, K15656; *ituA*, K15661). Functional groups enriched in Voltis bacterial communities are related to xenobiotic degradation (*nthB*, K20807; *ABC-2.A*, K01990; *mas*, K18481; *gctB*, K01040), antibiotic production (*chiA*, K13381; *cvpA*, K03558; bcsZ, K20542) and volatile compound metabolism (*fabL*, K10780; *fabI*, K00208; *atoB*, K00626).

By comparing the differentially abundant functions in healthy and *P. viticola*-infected untreated Chardonnay, several genes related to polyamine metabolism were identified as enriched in healthy plants. Four genes are related to a spermidine/putrescine import ABC transporter complex (*ABC.SP.P*, *ABC.SP.P1*, *ABC.SP.S*, K02053-54,55 and *potA*, K11072) and another to a putrescine-ornithine antiporter (*potE*, K03756). Other functions related to polyamine catabolism were also enriched, including a gamma-glutamylputrescine synthase (*puuA*, K09470), involved in the first step of conversion of putrescine to succinate, and a spermidine dehydrogenase (*spdH*, K00316), which catalyzes the oxidation of spermidine to 1,3-diaminopropane and Δ^1-pyrroline.

Functions associated with bacterial communities of non-infected plants are more stable than those found in untreated Chardonnay. In treated Chardonnay, only putrescine-ornithine antiporter (*potE*, K03756) and a putative tricarboxylic transport membrane protein (*tctB*, K07794) are enriched at flowering and veraison, respectively. In Voltis, no significant function enrichment was detected when comparing flowering and veraison stages.

Bacterial species assignment through the annotation of microbial assembled genomes

MAGs of interest and showing more than 60% of genome completion were annotated using the MicroScope plateform (Supplementary Tables S3, S4), and their identified functions were classified with EGGNOG (Supplementary Table S5). Functions enriched in the metagenome for which abundance varied according to cultivar and the presence or absence of *P. viticola* were searched for in the MAGs to establish a relationship between functions and taxa enriched in similar conditions (Tables 1 and 2). In absence of infection with *P. viticola*, functions enriched in bacterial community of untreated Chardonnay compared to Voltis, including lipopeptide synthesis (*srfAA*, K15654; *srfAC*, K15656; *ituA*, K15661), spermidine dehydrogenase (*spdH*, K00316), putrescine-ornithine antiporter (*potE*, K03756) and 4-guanidinobutyraldehyde dehydrogenase/NAD-dependent aldehyde dehydrogenase (*kauB*, K12254), are absent. In the same conditions some genes enriched in Voltis rhizosphere are not retrieved. These genes encode mainly Mce-associated membrane protein (*mas*, K18481) and glutaconate CoA-transferase, subunit B (*gctB*, K01040) associated with xenobiotic degradation, as well as enoyl-[acyl-carrier protein] reductase III (*fabL*, K10780), involved in volatile compound metabolism. However, it is not possible to discriminate the products of the *ABC.SP.P* and *ABC.SP.P1* genes (K02053; K02054).

Some genes are also enriched in healthy Chardonnay (compared to diseased Chardonnay) and the corresponding reconstructed MAGs. It is the case for genes involved in putrescine transport and degradation (*potA*, K11072 and *ABC.SP.P*, *ABC.SP.P1*, *ABC.SP.S*, K02053-55), enriched in the *Phyllobacterium* and *Pseudomonas* genomes of untreated Chardonnay in absence of *P. viticola*. These genes are also retrieved in the same bacterial genomes of treated Chardonnay and Voltis. Interestingly, the gene encoding gamma-glutamylputrescine synthase (*puuA*, K09470) is found only in a *Pseudomonas* genome. The deferrochelatase/peroxidase gene (*efeB*, K16301), enriched in the untreated Chardonnay compared to Voltis in absence of *P. viticola*, is found only in *Phyllobacterium* and *Pseudomonas* genomes. The genes encoding ABC-2 type transport system ATP-binding protein (*ABC-2.A*, K01990) and membrane protein required for colicin V production (*cvpA*, K03558) are retrieved in all the genomes originated from the Voltis at flowering. The only MAG containing *chitinase A* (*chiA*, K13381) is assigned to a *Flavobacterium* originated from the rhizosphere of infected Chardonnay (untreated at veraison). Differences in the number of coding sequences (CDS) are also noticed depending on the functions and microbial genomes. For example, *Variovorax* and *Acidovorax* MAGs contain many CDS associated to a putative tricarboxylic transport membrane protein (K07794). It is also worth noting that the number of CDS varies between MAGs of *Pseudomonas* and *Phyllobacterium* genera for functions associated to putrescine transport and degradation.

Discussion

Grapevines (*Vitis vinifera* L.) are highly susceptible to downy mildew caused by the oomycete *Plasmopara viticola* [56, 57]. Most vineyards rely on frequent fungicide treatments to limit disease propagation and yield losses. The breeding of mildew tolerant *Vitis vinifera* varieties integrating resistance genes from American and Asian *Vitis* species has been proposed as an alternative strategy [16]. However, adopting such resistant hybrids is still uncertain in terms of their sustainable resistance to *P. viticola* and other diseases. Recent studies have shed light on the functional role that rhizospheric or epiphytic microbiome may play in plant health and suggest that specific microbial taxa may contribute de systemic resistance to diseases [4, 58–60]. Here, we used deep

Table 1 Number of coding sequences in MAGs associated to the plant-beneficial functions shown as enriched in metagenomic analyses by comparing the voltis and Chardonnay at flowering. Gray cells indicate the functions enriched in the conditions the microorganisms are originated from (CNT = untreated Chardonnay; ct = treated Chardonnay; VOL = voltis; f = flowering; V = Veraison). Only functions supposed to be related to plant protection were searched. The functions not shown in the table were not found. A coding sequence was count when the gene of interest (*) or the associated product was observed

	Gene	**puuA**	**ABC.SP.P1 ydcU**	**efeB**	**cysI**	**nthB**	**ABC-2.A yadG**	**chiA yheB**	**cvpA**	**bcsZ yhjM**	**fabI**	**ACAT atoB**
	KEGG	K09470	K02054	K16301	K00381	K20807	K01990	K13381	K03558	K20542	K00208	K00626
Genus	Enriched in:	Untreated Chardonnay	Untreated Chardonnay	Untreated Chardonnay	Untreated Chardonnay	Voltis	Voltis	Voltis	Voltis	Voltis	Voltis	Voltis
Nitrosopumilales	CNTV_Bin7						2					
Nitrosopumilales	CTV_Bin3						2					
Flavobacterium	CNTV_Bin5						4	1	1	2		1
Shingobacterium	CNTF_Bin35						6			1		1
Shingobacterium	CTF_Bin39						6			2		1
Phyllobacterium	CNTF_Bin24		2	1*		1*			1	2	2*	
Phyllobacterium	CNTF_Bin39		8		1	1*			1		2*	
Phyllobacterium	CTF_Bin18		2	1*	1	1*			1	2	2*	
Agrobacterium	CTF_Bin22		2		1				1	1	2*	
Cutibacterium	VOLF_Bin13						4		1			
Novosphingobium	CNTV_Bin25				1		2					
Paraburkholderia	VOLF_Bin15		12		2	1	2		1		1*	
Pseudomonas	CNTF_Bin20	1*	1						1*			
Pseudomonas	CTF_Bin33		4	1*	2				1		1*	
Variovorax	CTV_Bin11		11				3		1		1*	1
Acidovorax	CNTV_Bin9		4		1		1		1			

Table 2 Number of coding sequences in MAGs associated to the plant-beneficial functions shown as enriched in metagenomic analyses by comparing the untreated Chardonnay at flowering (in absence of symptoms of P. viticola) and Veraison (in presence of symptoms of P. viticola). Gray cells indicate the functions enriched in the conditions the microorganisms are originated from (CNT = untreated Chardonnay; CT = treated Chardonnay; VOL = Voltis; F = Flowering; V = Veraison). Only functions supposed to be related to plant protection were searched. The functions not shown in the table were not found. A coding sequence was count when the gene of interest (*) or the associated product was observed

	Gene	**potA**	**puuA**	**ABC.SP.*P* ydcV**	**ABC.SP.P1 ydcU**	**ABC.SP.S ydcS**
	KEGG	K11072	K09470	K02053	K02054	K02055
Genus	Enriched at:	Flowering	Flowering	Flowering	Flowering	Flowering
Nitrosopumilales	CNTV_Bin7					
Nitrosopumilales	CTV_Bin3					
Flavobacterium	CNTV_Bin5					
Shingobacterium	CNTF_Bin35					
Shingobacterium	CTF_Bin39					
Phyllobacterium	CNTF_Bin24	3*		2	2	2
Phyllobacterium	CNTF_Bin39	7*		8	8	2
Phyllobacterium	CTF_Bin18	2*		2	2	2
Agrobacterium	CTF_Bin22	4*		2	2	2
Cutibacterium	VOLF_Bin13					
Novosphingobium	CNTV_Bin25					
Paraburkholderia	VOLF_Bin15	8*		12	12	6
Pseudomonas	CNTF_Bin20	3*	1*	1	1	
Pseudomonas	CTF_Bin33	3*		4	4	1
Variovorax	CTV_Bin11	2*		11	11	5
Acidovorax	CNTV_Bin9	2*		4	4	1

sequencing for a detailed characterization of bacterial diversity, structure and functions in the roots and rhizospheric soil of two grapevine cultivars with contrasted susceptibility to *P. viticola*, Chardonnay (susceptible) and Voltis (resistant interspecific hybrid), at flowering and veraison stages. In Champagne, the year 2021 was marked by climatic conditions highly propitious to downy mildew outbreaks. While downy mildew symptoms were not detected at flowering stage, its late onset at veraison caused severe damage on susceptible untreated Chardonnay, but not on Voltis and fungicide-treated Chardonnay. Analysis of spatial rhizocompartments provided new insights into distinct and overlapping bacterial assemblies and functions in the rhizospheric soil, rhizoplane and root endosphere, depending on grapevine cultivar and its health status with regard to downy mildew. It also highlighted the presence of *Candidatus* Phytoplasma in the endosphere of both cultivars, which is responsible for Bois Noir and Flavescence dorée. This may suggest that this pathogen can colonize the root system without inducing any damage, as no symptoms of Bois Noir or Flavescence Dorée have been observed at flowering or veraison stages. The lack of symptoms, which could be due to a low expression of pathogenic effectors, and the persistence of this pathogen in recovered plants, suggest that downy mildew may be considered as prevalent on the observed microbiome changes [61, 62]. Although the metagenomic analyses showed a very relative presence of sequences associated with fungi, the most significant results were seen in the bacteriome.

Rhizospheric soil and rhizoplane shared common bacterial functions in both susceptible and resistant cultivars despite different bacterial communities

In this study, we showed a commonly shared bacteriome core between susceptible and resistant cultivars, with a particular dominance of Proteobacteria, followed by Actinobacteria, Bacteroidota, Firmicutes, Acidobacteriota and Verrucomicrobiota. This is consistent with previous observations of root-associated microbial communities of rootstock genotypes [58], and suggests convergent functional traits between the rhizosphere and rhizoplane bacteriomes in both susceptible and resistant cultivars. Nevertheless, although Proteobacteria are abundant in all plant parts, other bacterial taxa seem to be more specific to each rhizocompartment. The rhizosphere is colonized preferentially by Actinobacteria and Acidobacteriota, while the endosphere harbors Bacteroidota and Firmicutes in both susceptible and resistant varieties. Methylomirabilota, on the other hand, seem to be preferentially associated with the sensitive variety at both flowering and veraison stages, and could be considered as relevant bioindicators and predictive of disease outcomes. This is line with Gu et al. [63] who reported that changes in the rhizosphere community composition rather than the overall species diversity can explain future plant health. To the best of our knowledge, this

study constitutes the first evidence of distinct rhizocompartment bacteriomes in downy mildew-susceptible and resistant grapevine cultivars.

When rhizocompartments were grouped, the dynamic of bacteriome assembly (from flowering to veraison) showed opposite trends in susceptible and resistant varieties. A reduction in the proportion of Proteobacteria and Bacteroidota, and an increase in Actinobacteria were observed in Chardonnay and inversely in Voltis. The contrasting dynamics of the rhizosphere microbiome composition of the two grape varieties could result from a difference in genetic background or from shifts in root exudation profiles following pathogen challenge, and therefore from interactions between the root system and the soil microbiome. The increased abundance of Actinobacteria in the rhizosphere of susceptible cultivar could support their potential role as mediators of plant health as reported earlier [64].

Despite differences in microbial populations between grape cultivars, the untreated Chardonnay and Voltis shared common functions in both rhizoplane and rhizospheric soil. This observation highlighted some functions with predicted importance for root colonization and establishment of microbial populations [65–71]. Indeed, in susceptible plants (untreated Chardonnay) genes involved in symbiosis and biofilm formation (*fabG; expr; roe*) were found in rhizoplane bacteria, while in rhizospheric soil, genes involved in biofilm production and root colonization (*purB*, *PilJ* and *ubiD*) were detected. The presence of *acrA* (associated to a resistance to β-lactam and cationic antimicrobial peptide) in the rhizoplane indicates the possibility of a competition between the microorganisms to colonize this niche [72]. The enrichment in rhizospheric soil of several genes involved in DNA recombination, replication and repair may originate from bacteria with larger genomes, adapted to changing and stressful environments [73, 74]. Although Voltis and untreated Chardonnay share most functions in both rhizoplane and rhizospheric soil, some specificities were found in the Voltis rhizoplane, as more genes are involved in stress tolerance and antibiotic resistance. Interestingly, *chvG* gene also associated to β-lactam resistance, like *acrA* in untreated Chardonnay, is more present in Voltis rhizoplane, suggesting a common interspecies competition against β-lactam producers [75].

Rhizospheric microbiome composition may be determined by the host's susceptibility to downy mildew

We observed a strong shift in bacterial diversity with the onset of downy mildew disease for the susceptible cultivar (untreated Chardonnay). In Voltis, which is highly resistant to downy mildew, the root bacterial communities remained stable. Enrichment analyzes showed that *Pseudomonas*, *Sphingobacterium*, *Phyllobacterium*, *Allorhizobium*, *Neorhizobium*, *Pararhizobium*, *Rhizobium*, *Chryseobacterium* and *Arthrobacter* are the main genera concerned by the reduction in bacterial diversity observed from flowering to veraison in the highly *P. viticola*-infected cultivar, Chardonnay. Such a reduction was offset at veraison through an increase in population evenness and total diversity of observed bacteria. Thus, the state of the bacteriome composition can probably reflect initial divergences between the sensitive and resistant grape varieties in the assembly of the microbial community.

It is worth noting that the untreated Chardonnay has never been subjected to pesticide treatments since planting and is yearly damaged by downy mildew infections. The microbial composition of its rhizosphere is dominated by few bacterial genera, resembling a specialized microbiome tailored by specific root exudates. This prevalence of a reduced number of taxa could also be the result of a soil-born legacy, wherein the Chardonnay microbiome would be shaped by successive pathogen infections [76]. Interestingly, the taxa enriched in healthy Chardonnay at flowering are dominantly recognized for their plant growth/health promoting potential. For instance, *Phyllobacterium* species are known for their rhizobial activities and are therefore able to freely fix nitrogen and promote plant growth and root architecture [77–79]. *Pseudomonas* species are also amongst the earliest agents involved in plant growth promotion and priming plants for enhanced systemic immunity [18, 80–82]. In particular, some strains of *Pseudomonas fluorescens* have been shown to improve grapevine resistance response against *P. viticola* [20, 83]. *Chryseobacterium* species have been repeatedly isolated from plant environments and show a large panel of beneficial activities ranging from antibiotic production to phosphate solubilization [84–86]. Similarly, the bacteria from the *Allorhizobium-Neorhizobium-Pararhizobium-Rhizobium* group are mainly known for their symbiosis with legumes and their biostimulation and biocontrol activities [87]. In addition, *Sphingobacterium* and *Arthrobacter* have been characterized by their ability to increase host tolerance to diverse abiotic stress such as salt, drought or cold [88–92]. Still, these taxa have also raised interest for their ability to promote plant growth and protection against diseases through pathogen antagonism, phosphate solubilization and auxin production [93–95]. This suggests that, despite their susceptibility to disease, certain grape varieties such as Chardonnay can maintain a microbial community rich in beneficial species that can contribute to the plant health.

Although there are more taxa enriched in the rhizosphere of Voltis at flowering, only few (*Bradyrhizobium*, *Streptomyces*, *Pantoea*) can be directly linked to plant

beneficial activities and could thus be predictive of a good plant health status [63]. *Bradyrhizobium* and *Streptomyces* taxa are known to promote plant growth and defense and prime symbiosis formation [85–87, 96–98]. Similarly, some *Pantoea* spp. have also been identified as biocontrol agents through direct antagonism or stimulation of plant innate immunity [19, 99]. Voltis is enriched in non-specialist taxa such as *Steroidobacter*, *Polaromonas*, *Reyranella* or *Vicinamibacteriaceae*. Interestingly, when focusing on the most abundant taxa at the species level, the susceptible cultivar (untreated Chardonnay) displays a more diverse bacterial community at flowering than the resistant one (Voltis). Since the assembly of sequences from shotgun metagenomics requires a high number of reads from the same species, we focused on the fifty longest assemblies. This results in a bias towards the dominant taxa within the bacterial communities. Nevertheless, the results are corroborated by the metabarcoding analysis, revealing a dominance of various species belonging to *Pseudomonas fluorescens* group and other beneficial taxa, including *Paraburkholderia*, *Sphingobacterium* and *Phyllobacterium* known for their plant growth promoting activities [88, 100, 101]. At veraison however, the diversity of dominant species found in MAGs was less important and consisted mainly of the pathogenic *Agrobacterium rhizogenes* (from 2% of MAGs at flowering to 58% at veraison).

Our results also showed a shift in bacterial diversity in the susceptible cultivar Chardonnay, which tends to converge towards Voltis-community structures after *P. viticola* challenge at veraison. Moreover, genomic assemblies indicate that the most abundant rhizosphere-associated bacteria undergo a similar shift towards pathogenic species in both treated and untreated Chardonnay at veraison. The functional patterns associated with the rhizosphere communities display more plant-associated features in healthy untreated Chardonnay than in the other plant categories. In the resistant cultivar, the most abundant bacterial taxa showed a high stability between flowering and veraison, particularly in the rhizoplane and rhizosphere compartments. Overall, these observations indicate a substantial decline of root-associated bacteriome in the susceptible plants after pathogen infection. This decline can be attributed to a gradual microbial dysbiosis, as shown in the rhizosphere of declining vines [102] and Citrus in response to the aerial huanglongbing disease [103]. This supports the hypothesis of the ability of susceptible cultivars to regulate their microbial community during the onset of downy mildew, whereas the stability of the Voltis microbiome could be determined initially by its genetic traits and basal resistance to downy mildew. This dynamic can explain the increased similarity in root bacteriome between susceptible and resistant cultivars after pathogen challenge at veraison. The observed dysbiosis is therefore characterized by a gain of community, in correlation with the increased Shannon index at veraison, resulting in a shift in the relative abundance of microbes and ultimately to a reduction in the more abundant beneficials at flowering.

Functional signatures in the rhizosphere are linked to plant immunity

While the functional shift occurring in the root communities of untreated Chardonnay with the onset of disease is largely conserved in Voltis, the latter exhibits an additional and specific enrichment of functions. For instance, the enrichment of functions associated with cell metabolism in the rhizospheric soil could suggest an increased metabolic versatility, which is consistent with the higher bacterial diversity observed in the rhizosphere of Voltis. However, these functional attributes are almost absent in treated Chardonnay in response to disease exposure. This is also evidenced by the relative stability of its rhizosphere community composition throughout the seasons. It is thus likely that agrochemical application is impairing the plant's ability to influence its microbiota. Agrochemicals could affect directly the soil microbiome or indirectly by impacting the synthesis of roots exudates needed for the appropriate microbiome recruitment, or by preventing plant-pathogen interactions, which are essential for the recruitment of a specific and even beneficial microbiota [104]. This observation is consistent with the similarly between functional enrichment of treated plants and bacterial abundance in rhizocompartments.

Despite a larger taxonomic diversity in the Voltis rhizosphere at flowering, we found more functional enrichments in the untreated Chardonnay. Overall, 19 genes were significantly enriched in the Chardonnay rhizosphere, whereas 14 genes were more abundant in the Voltis rhizosphere at flowering. Functional groups identified in Chardonnay are related to putrescine transport and putrescine degradation, iron acquisition and lipopeptide synthesis. However, functional groups enriched in Voltis bacterial communities are related to xenobiotic degradation, antibiotic synthesis and volatile compound metabolism. These distinct functional enrichments between cultivars suggest that the select species enriched in the susceptible cultivar bring along a consistent set of functions compared to resistant plants. The enrichment of functions involved in putrescine transport and degradation suggests that the plant may use this metabolite to attract specific communities able to uptake and use this polyamine as a nitrogen and carbon source [105]. The role of putrescine in plant-bacteria dialogue and as a signaling molecule in the rhizosphere has also been reported [106, 107]. Putrescine uptake by the beneficial bacterium *Pseudomonas fluorescens* WCS365 was shown to be finely regulated and involved in root colonization

through the promotion of biofilm [105, 106]. This is in line with the abundance of *Pseudomonas* in the rhizosphere of untreated Chardonnay at flowering. The putrescine degradation is also involved in metabolic flux through the formation of γ-aminobutyric acid (GABA), which is considered as a key defense-related metabolite [108]. This is also consistent with the annotated MAGs indicating the presence of the *puuA* gene encoding a gamma-glutamylputrescine synthase, involved in GABA production, once in a *Pseudomonas* genome from Chardonnay in absence of *P. viticola*. The analysis of MAGs in this manuscript therefore represents a novel approach to the study of diseased plant/microbiome interactions and enables us to decipher the mechanisms at the genome level of each individual.

The enrichment of genes associated to polyamine transport and catabolism in the rhizosphere of healthy untreated Chardonnay indicates the host's ability to select bacteria with plant-beneficial traits. Overall, these functions were retrieved in the MAGs of Gammaproteobacteria and Alphaproteobacteria genera, and more particularly in the *Pseudomonas* and *Phyllobacterium* genera enriched in the rhizosphere healthy untreated Chardonnay. Putrescine transporters such as *ydcS* and *ydcV* were also suggested to play a role in double-stranded DNA uptake, promoting horizontal gene transfer [109]. The concurrent enrichment of *mrr*, an endonuclease targeting foreign methylated DNA [110], further suggests the presence of active bacterial community in the rhizosphere of untreated Chardonnay. Moreover, several functions enriched in healthy untreated Chardonnay compared to Voltis may be involved in the induction of plant immunity, such as genes encoding the biosynthesis of lipopeptides, iturins and surfactin, usually produced by *Bacillus* species [111]. These genes were not retrieved in the annotated MAGs, meaning they could belong to other enriched genera. Moreover, the detection of *cysI*, a subunit of a sulfite reductase which can catalyze the reduction of several siderophores [112] and *efeB*, a protein allowing the transport of ferric and ferrous iron could reflect the ability of some bacteria to modulate the plant resistance by reducing iron availability [113, 114]. Both functional genes were retrieved only in *Phyllobacterium* and *Pseudomonas* MAGs from the susceptible plants. Thus, the healthy untreated Chardonnay, compared to the resistant cultivar, might exert a selection pressure of microbial populations with plant-beneficial functions associated with pathogen control and the induction of plant immunity.

Conclusions

Overall, this study provided new insights into distinct and overlapping bacterial communities and functions in the rhizospheric soil, rhizoplane and root endosphere of both susceptible and resistant cultivars. Both cultivars are sharing a bacteriome core and common gene enrichments involved in root colonization in the rhizoplane and rhizospheric soil. The susceptible cultivar displays an enrichment of beneficial taxa negatively impacted by *P. viticola* infection. This is associated with a loss of predicted functions related to plant immunity induction, which can reveal a gradual microbial dysbiosis. Thus, the corresponding taxa could be isolated to explore their potential in the induction of grapevine immunity against *P. viticola*. The rhizosphere of resistant cultivar exhibits mainly non-specialist taxa and functions, maintained during disease onset, that can be determined by its genetic basal resistance. However, the role of the rhizomicrobiome remains to be clarified through transcriptomic and metabolomic studies, as changes in the metagenome are not fully representative of variations occurring in the microbial metabolic activities.

Supplementary Information

The online version contains supplementary material available at https://doi.org/10.1186/s40793-025-00690-w.

Supplementary Material 1

Acknowledgements
We thank the Committee Champagne for providing us with experimental plots and for their assistance for sampling.

Author contributions
A.A., MD and AW conceived and designed the research. M.D., A.W. and A.A. performed the experiments. A.W., M.D. and L.B. analyzed the data. A.A. supervised the research. M.D. and A.W. wrote the original draft. A.A. revised and edited the manuscript. All authors read and approved the manuscript.

Funding
This research was supported by the French National Research Agency through the PRIMA-MiDiVine project, Grant N° 1564.

Data availability
Sequence data that support the findings of this study have been deposited in the NCBI with the primary accession code (BioProject ID): PRJNA1162681.

Declarations

Ethics approval and consent to participate
Not applicable.

Consent for publication
Not applicable.

Competing interests
The authors declare no competing interests.

Author details
[1]Université de Reims Champagne-Ardenne, INRAE, RIBP, USC 1488, Reims 51100, France
[2]Université de Reims Champagne-Ardenne, INRAE, FARE, UMR A 614, Reims 51100, France

Received: 30 August 2024 / Accepted: 23 February 2025
Published online: 14 March 2025

References

1. Leach JE, Triplett LR, Argueso CT, Trivedi P. Communication Phytobiome Cell. 2017;169:587–96.
2. Bulgarelli D, Schlaeppi K, Spaepen S, Van Themaat EVL, Schulze-Lefert P. Structure and functions of the bacterial microbiota of plants. Annu Rev Plant Biol. 2013;64:807–38.
3. Beilsmith K, Thoen MPM, Brachi B, Gloss AD, Khan MH, Bergelson J. Genome-wide association studies on the phyllosphere microbiome: embracing complexity in host–microbe interactions. Plant J. 2019;97:164–81.
4. Pacifico D, Squartini A, Crucitti D, Barizza E, Lo Schiavo F, Muresu R et al. The role of the endophytic Microbiome in the grapevine response to environmental triggers. Front Plant Sci. 2019;10:1256. https://doi.org/10.3389/fpls.2019.01256.
5. Lau JA, Lennon JT. Rapid responses of soil microorganisms improve plant fitness in novel environments. Proc Natl Acad Sci U S A. 2012;109:14058–62.
6. Mendes R, Kruijt M, De Bruijn I, Dekkers E, Van Der Voort M, Schneider JHM, et al. Deciphering the rhizosphere Microbiome for disease-suppressive bacteria. Science. 2011;332:1097–100.
7. Kwak MJ, Kong HG, Choi K, Kwon SK, Song JY, Lee J, et al. Rhizosphere Microbiome structure alters to enable wilt resistance in tomato. Nat Biotechnol. 2018;36:1100–16.
8. Li JH, Muhammad Aslam M, Gao YY, Dai L, Hao GF, Wei Z, et al. Microbiome-mediated signal transduction within the plant holobiont. Trends Microbiol. 2023;31:616–28.
9. Pieterse CMJ, Zamioudis C, Berendsen RL, Weller DM, Van Wees SCM, Bakker PAHM. Induced systemic resistance by beneficial microbes. Annu Rev Phytopathol. 2014;52:347–75.
10. Wei Z, Gu Y, Friman VP, Kowalchuk GA, Xu Y, Shen Q, et al. Initial soil Microbiome composition and functioning predetermine future plant health. Sci Adv. 2019;5:759–84.
11. Wagner MR, Lundberg DS, Del Rio TG, Tringe SG, Dangl JL, Mitchell-Olds T. Host genotype and age shape the leaf and root microbiomes of a wild perennial plant. Nat Commun 2016 71. 2016;7:1–15.
12. Grady KL, Sorensen JW, Stopnisek N, Guittar J, Shade A. Assembly and seasonality of core phyllosphere microbiota on perennial biofuel crops. Nat Commun 2019 101. 2019;10:1–10.
13. Berendsen RL, Vismans G, Yu K, Song Y, De Jonge R, Burgman WP, et al. Disease-induced assemblage of a plant-beneficial bacterial consortium. ISME J 2018 126. 2018;12:1496–507.
14. FAO. FAO publications catalogue 2023. http://www.fao.org/home/fr. Accessed 18 Nov 2023.
15. Pertot I, Caffi T, Rossi V, Mugnai L, Hoffmann C, Grando MS, et al. A critical review of plant protection tools for reducing pesticide use on grapevine and new perspectives for the implementation of IPM in viticulture. Crop Prot. 2017;97:70–84.
16. Schneider C, Onimus C, Prado E, Dumas V, Wiedemann-Merdinoglu S, Dorne MA, et al. INRA-ReSDUR: the French grapevine breeding programme for durable resistance to downy and powdery mildew. Acta Hortic. 2019;1248:207–13.
17. Pinto C, Pinho D, Sousa S, Pinheiro M, Egas C, Gomes AC. Unravelling the diversity of grapevine Microbiome. PLoS ONE. 2014;9:85622.
18. Gruau C, Trotel-Aziz P, Villaume S, Rabenoelina F, Clement C, Baillieul F, et al. Pseudomonas fluorescens PTA-CT2 triggers local and systemic immune response against Botrytis cinerea in grapevine. Mol Plant-Microbe Interact. 2015;28:1117–29.
19. Aziz A, Verhagen B, Magnin-Robert M, Couderchet M, Clément C, Jeandet P et al. Effectiveness of beneficial bacteria to promote systemic resistance of grapevine to Gray mold as related to phytoalexin production in vineyards on JSTOR. Plant Soil. 2016;405:141–53. https://doi.org/10.1007/s11104-015-2783-z.
20. Lakkis S, Trotel-Aziz P, Rabenoelina F, Schwarzenberg A, Nguema-Ona E, Clément C, et al. Strengthening grapevine resistance by Pseudomonas fluorescens PTA-CT2 relies on distinct defense pathways in susceptible and partially resistant genotypes to downy mildew and Gray mold diseases. Front Plant Sci. 2019;10:1112.
21. Trotel-Aziz P, Abou-Mansour E, Courteaux B, Rabenoelina F, Clément C, Fontaine F et al. Bacillus subtilis PTA-271 counteracts Botryosphaeria dieback in grapevine, triggering immune responses and detoxification of fungal phytotoxins. Front Plant Sci. 2019;10: 25. https://doi.org/10.3389/fpls.2019.00025.
22. Deyett E, Rolshausen PE. Endophytic microbial assemblage in grapevine. FEMS Microbiol Ecol. 2020;96:53.
23. Fotios B, Sotirios V, Elena P, Anastasios S, Stefanos T, Danae G, et al. Grapevine wood Microbiome analysis identifies key fungal pathogens and potential interactions with the bacterial community implicated in grapevine trunk disease appearance. Environ Microbiome 2021 161. 2021;16:1–17.
24. Arnault G, Mony C, Vandenkoornhuyse P. Plant microbiota dysbiosis and the Anna karenina principle. Trends Plant Sci. 2023;28:18–30. https://doi.org/10.1016/j.tplants.2022.08.012.
25. Liu H, Brettell LE, Qiu Z, Singh BK. Microbiome-Mediated stress resistance in plants. Trends Plant Sci. 2020;25:733–43.
26. Barroso-Bergadà D, Delmotte F, d'Arcier JF, Massot M, Chancerel E, Demeaux I et al. Leaf Microbiome Data for European Cultivated Grapevine (Vitis vinifera) During Downy Mildew (Plasmopara viticola) Epidemics in Three Wine-Producing Regions in France. https://doi.org/101094/PHYTOFR-11-22-*.0138-A* 2023; X, No. X.
27. Zhang S, Wang Y, Chen X, Cui B, Bai Z, Zhuang G. Variety features differentiate microbiota in the grape leaves. Can J Microbiol. 2020;66:653–63.
28. Singh P, Santoni S, This P, Péros JP. Genotype-Environment interaction shapes the microbial assemblage in grapevine's phyllosphere and Carposphere: an NGS approach. Microorganisms 2018;6:96. https://doi.org/10.3390/microorganisms6040096.
29. Fort T, Robin C, Capdevielle X, Delière L, Vacher C. Foliar fungal communities strongly differ between habitat patches in a landscape mosaic. *PeerJ* 2016; 4.
30. Liu D, Howell K. Community succession of the grapevine fungal Microbiome in the annual growth cycle. Environ Microbiol. 2021;23:1842–57.
31. Yang H-C, Rodriguez-Ramos JC, Hale L, Naegele RP. Grapevine Leaf Epiphytic Fungal and Bacterial Communities Are Influenced More by Spatial and Temporal Factors than by Powdery Mildew Fungicide Spray Programs. https://doi.org/101094/PHYTOFR-02-23-0012.-*R* 2024.
32. Perazzolli M, Palmieri MC, Matafora V, Bachi A, Pertot I. Phosphoproteomic analysis of induced resistance reveals activation of signal transduction processes by beneficial and pathogenic interaction in grapevine. J Plant Physiol. 2016;195:59–72.
33. Edwards J, Santos-Medellín C, Sundaresan V. Extraction and 16S rRNA sequence analysis of microbiomes associated with rice roots. BIO-PROTOCOL 2018;8:e2884. https://doi.org/10.21769/BioProtoc.2884.
34. Klindworth A, Pruesse E, Schweer T, Peplies J, Quast C, Horn M, et al. Evaluation of general 16S ribosomal RNA gene PCR primers for classical and next-generation sequencing-based diversity studies. Nucleic Acids Res. 2013;41:e1–1.
35. Chen S, Zhou Y, Chen Y, Gu J. Fastp: an ultra-fast all-in-one FASTQ preprocessor. Bioinformatics. 2018;34:i884–90.
36. Patz S, Gautam; B,; R,; R-P,,, Huson P. PLaBAse: A comprehensive web resource for analyzing the plant growth-promoting potential of plant-associated bacteria. *bioRxiv* 2021.
37. Gautam A, Felderhoff H, Bağci C, Huson DH. Using AnnoTree to Get More Assignments, Faster, in DIAMOND + MEGAN Microbiome Analysis. *mSystems* 2022; 7.
38. Mendler K, Chen H, Parks DH, Lobb B, Hug LA, Doxey AC. AnnoTree: visualization and exploration of a functionally annotated microbial tree of life. Nucleic Acids Res. 2019;47:4442–8.
39. Buchfink B, Reuter K, Drost HG. Sensitive protein alignments at tree-of-life scale using DIAMOND. Nat Methods 2021 184. 2021;18:366–8.
40. Menzel P, Ng KL, Krogh A. Fast and sensitive taxonomic classification for metagenomics with Kaiju. Nat Commun 2016 71. 2016;7:1–9.
41. Li D, Liu C-M, Luo R, Sadakane K, Lam T-W. MEGAHIT: an ultra-fast single-node solution for large and complex metagenomics assembly via succinct de Bruijn graph. Bioinformatics. 2015;31:1674–6.
42. Altschul SF, Gish W, Miller W, Myers EW, Lipman DJ. Basic local alignment search tool. J Mol Biol. 1990;215:403–10.
43. Parks DH, Imelfort M, Skennerton CT, Hugenholtz P, Tyson GW. CheckM: assessing the quality of microbial genomes recovered from isolates, single cells, and metagenomes. Genome Res. 2015;25:1043–55.
44. Chaumeil P-A, Mussig AJ, Hugenholtz P, Parks DH. GTDB-Tk v2: memory friendly classification with the genome taxonomy database. Bioinformatics. 2022;38:5315–6.
45. Vallenet D, Engelen S, Mornico D, Cruveiller S, Fleury L, Lajus A et al. MicroScope: a platform for microbial genome annotation and comparative genomics. *Database* 2009; 2009.
46. Bolyen E, Rideout JR, Dillon MR, Bokulich NA, Abnet CC, Al-Ghalith GA, et al. Reproducible, interactive, scalable and extensible Microbiome data science using QIIME 2. Nat Biotechnol 2019 378. 2019;37:852–7.

47. Martin M. Cutadapt removes adapter sequences from high-throughput sequencing reads. EMBnet J. 2011;17:10–2.
48. Callahan BJ, McMurdie PJ, Rosen MJ, Han AW, Johnson AJA, Holmes SP. DADA2: high resolution sample inference from illumina amplicon data. Nat Methods. 2016;13:581.
49. Bokulich NA, Kaehler BD, Rideout JR, Dillon M, Bolyen E, Knight R, et al. Optimizing taxonomic classification of marker-gene amplicon sequences with QIIME 2's q2-feature-classifier plugin. Microbiome. 2018;6:1–17.
50. Glöckner FO, Yilmaz P, Quast C, Gerken J, Beccati A, Ciuprina A, et al. 25 Years of serving the community with ribosomal RNA gene reference databases and tools. J Biotechnol. 2017;261:169–76.
51. Katoh K, Misawa K, Kuma KI, Miyata T. MAFFT: a novel method for rapid multiple sequence alignment based on fast fourier transform. Nucleic Acids Res. 2002;30:3059–66.
52. Price MN, Dehal PS, Arkin AP. FastTree 2 – Approximately Maximum-Likelihood trees for large alignments. PLoS ONE. 2010;5:e9490.
53. Davis NM, Proctor DM, Holmes SP, Relman DA, Callahan BJ. Simple statistical identification and removal of contaminant sequences in marker-gene and metagenomics data. Microbiome. 2018;6:1–14.
54. McMurdie PJ, Holmes S. Phyloseq: an R package for reproducible interactive analysis and graphics of Microbiome census data. PLoS ONE. 2013;8:e61217.
55. Segata N, Izard J, Waldron L, Gevers D, Miropolsky L, Garrett WS, et al. Metagenomic biomarker discovery and explanation. Genome Biol. 2011;12:1–18.
56. Fontaine MC, Labbé F, Dussert Y, Delière L, Richart-Cervera S, Giraud T, et al. Europe as a bridgehead in the worldwide invasion history of grapevine downy mildew, Plasmopara viticola. Curr Biol. 2021;31:2155–e21664.
57. Gouveia C, Santos RB, Paiva-Silva C, Buchholz G, Malhó R, Figueiredo A. The pathogenicity of Plasmopara viticola: a review of evolutionary dynamics, infection strategies and effector molecules. BMC Plant Biol. 2024;24:327. https://doi.org/10.1186/s12870-024-05037-0.
58. Gao M, Xiong C, Gao C, Tsui CKM, Wang MM, Zhou X, et al. Disease-induced changes in plant Microbiome assembly and functional adaptation. Microbiome 2021 91. 2021;9:1–18.
59. Liu T, Xiao Y, Yin J, Yi T, Zhou Z, Hsiang T, et al. Effects of cultured root and soil microbial communities on the disease of Nicotiana tabacum caused by Phytophthora nicotianae. Front Microbiol. 2020;11:534330.
60. Trivedi P, Mattupalli C, Eversole K, Leach JE. Enabling sustainable agriculture through Understanding and enhancement of microbiomes. New Phytol. 2021;230:2129–47.
61. Landi L, Murolo S, Romanazzi G. Detection of'candidatus Phytoplasma Solani' in roots from bois Noir symptomatic and recovered grapevines. Sci Rep 2019 91. 2019;9:1–12.
62. Darriaut R, Lailheugue V, Masneuf-Pomarède I, Marguerit E, Martins G, Compant S et al. Grapevine rootstock and soil Microbiome interactions: keys for a resilient viticulture. Hortic Res 2022; 9.
63. Gu Y, Banerjee S, Dini-Andreote F, Xu Y, Shen Q, Jousset A, et al. Small changes in rhizosphere Microbiome composition predict disease outcomes earlier than pathogen density variations. ISME J 2022 1610. 2022;16:2448–56.
64. Álvarez-Pérez JM, González-García S, Cobos R, Olego MÁ, Ibañez A, Díez-Galán A et al. Use of endophytic and rhizosphere actinobacteria from grapevine plants to reduce nursery fungal graft infections that lead to young grapevine decline. Appl Environ Microbiol. 2017;83(24):e01564-17. https://doi.org/10.1128/AEM.01564-17.
65. Shanbhag AP. FabG: from a core to circumstantial catalyst. Biotechnol Lett. 2019;41:675–88.
66. Nogales J, Bernabéu-Roda L, Cuéllar V, Soto MJ. ExpR is not required for swarming but promotes sliding in sinorhizobium meliloti. J Bacteriol. 2012;194:2027–35.
67. Pellock BJ, Teplitski M, Boinay RP, Bauer WD, Walker GC. A LuxR homolog controls production of symbiotically active extracellular polysaccharide II by Sinorhizobium meliloti. J Bacteriol. 2002;184:5067–76.
68. Patankar AV, González JE. An orphan LuxR homolog of Sinorhizobium meliloti affects stress adaptation and competition for nodulation. Appl Environ Microbiol. 2009;75:946–55.
69. Merritt JH, Ha DG, Cowles KN, Lu W, Morales DK, Rabinowitz J et al. Specific control of Pseudomonas aeruginosa surface-associated behaviors by two c-di-GMP diguanylate cyclases. *MBio* 2010; 1.
70. Chauhan PS, Nautiyal CS. The purb gene controls rhizosphere colonization by Pantoea agglomerans. Lett Appl Microbiol. 2010;50:205–10.
71. Persat A, Inclan YF, Engel JN, Stone HA, Gitai Z. Type IV pili mechanochemically regulate virulence factors in Pseudomonas aeruginosa. Proc Natl Acad Sci U S A. 2015;112:7563–8.
72. Abdali N, Parks JM, Haynes KM, Chaney JL, Green AT, Wolloscheck D, et al. Reviving antibiotics: efflux pump inhibitors that interact with AcrA, a membrane fusion protein of the AcrAB-TolC multidrug efflux pump. ACS Infect Dis. 2017;3:89–98.
73. Touchon M, Rocha EPC. Causes of insertion sequences abundance in prokaryotic genomes. Mol Biol Evol. 2007;24:969–81.
74. Vigil-Stenman T, Ininbergs K, Bergman B, Ekman M. High abundance and expression of transposases in bacteria from the Baltic sea. ISME J. 2017;11:2611.
75. Bucher T, Keren-Paz A, Hausser J, Olender T, Cytryn E, Kolodkin-Gal I. An active β-lactamase is a part of an orchestrated cell wall stress resistance network of Bacillus subtilis and related rhizosphere species. Environ Microbiol. 2019;21:1068–85.
76. Yuan J, Zhao J, Wen T, Zhao M, Li R, Goossens P et al. Root exudates drive the soil-borne legacy of aboveground pathogen infection. Microbiome. 2018;6:156. https://doi.org/10.1186/s40168-018-0537-x.
77. Kechid M, Desbrosses G, Rokhsi W, Varoquaux F, Djekoun A, Touraine B. The NRT2.5 and NRT2.6 genes are involved in growth promotion of Arabidopsis by the plant growth-promoting rhizobacterium (PGPR) strain Phyllobacterium brassicacearum STM196. New Phytol. 2013;198:514–24.
78. Bertrand H, Nalin R, Bally R, Cleyet-Marel JC. Isolation and identification of the most efficient plant growth-promoting bacteria associated with Canola (Brassica napus). Biol Fertil Soils. 2001;33:152–6.
79. Mantelin S, Desbrosses G, Larcher M, Tranbarger TJ, Cleyet-Marel JC, Touraine B. Nitrate-dependent control of root architecture and N nutrition are altered by a plant growth-promoting Phyllobacterium Sp. Planta. 2006;223:591–603.
80. Backer R, Rokem JS, Ilangumaran G, Lamont J, Praslickova D, Ricci E, et al. Plant Growth-Promoting rhizobacteria: context, mechanisms of action, and roadmap to commercialization of biostimulants for sustainable agriculture. Front Plant Sci. 2018;9:1473.
81. Santoyo G, Orozco-Mosqueda M, del Govindappa C. Mechanisms of biocontrol and plant growth-promoting activity in soil bacterial species of Bacillus and Pseudomonas: a review. Biocontrol Sci Technol. 2012;22:855–72.
82. Silby MW, Cerdeño-Tárraga AM, Vernikos GS, Giddens SR, Jackson RW, Preston GM, et al. Genomic and genetic analyses of diversity and plant interactions of Pseudomonas fluorescens. Genome Biol. 2009;10:R51.
83. Archana S, Prabakar K, Raguchander T, Hubballi M, Valarmathi P, Prakasam V. Defense response of grapevine to Plasmopara viticola induced by azoxystrobin and Pseudomonas fluorescens. Int J Sustain Agric. 2011;3:30–8.
84. Singh AV, Chandra R, Goel R. Phosphate solubilization by Chryseobacterium Sp. and their combined effect with N and P fertilizers on plant growth promotion. Arch Agron Soil Sci. 2012;59:641–51. https://doi.org/10.1080/03650340.2012.664767.
85. Chhetri G, Kim I, Kim J, So Y, Seo T. Chryseobacterium tagetis sp. nov., a plant growth promoting bacterium with an antimicrobial activity isolated from the roots of medicinal plant (Tagetes patula). *J Antibiot* 2022 756 2022; 75: 312–320.
86. Montero-Calasanz M, del Göker C, Rohde M, Spröer M, Schumann C, Busse P. Chryseobacterium hispalense Sp. nov., a plantgrowth- promoting bacterium isolated from a rainwater pond in an Olive plant nursery, and emended descriptions of Chryseobacterium defluvii, Chryseobacterium indologenes, Chryseobacterium wanjuense and Chryseob. Int J Syst Evol Microbiol. 2013;63:4386–95.
87. Gopalakrishnan S, Sathya A, Vijayabharathi R, Varshney RK, Gowda CLL, Krishnamurthy L. Plant growth promoting rhizobia: challenges and opportunities. 3 Biotech. 2015;5:355–77.
88. Vaishnav A, Singh J, Singh P, Rajput RS, Singh HB, Sarma BK. Sphingobacterium Sp. BHU-AV3 induces salt tolerance in tomato by enhancing antioxidant activities and energy metabolism. Front Microbiol. 2020;11:443.
89. Khan MA, Ullah I, Waqas M, Hamayun M, Khan AL, Asaf S, et al. Halo-tolerant rhizospheric Arthrobacter woluwensis AK1 mitigates salt stress and induces physio-hormonal changes and expression of GmST1 and GmLAX3 in soybean. Symbiosis. 2019;77:9–21.
90. Hagaggi NSA, Abdul-Raouf UM. Drought-tolerant Sphingobacterium Changzhouense Alv associated with Aloe vera mediates drought tolerance in maize (Zea mays). World J Microbiol Biotechnol. 2022;38:248.
91. Krishnan R, Menon RR, Tanaka N, Busse H-J, Krishnamurthi S, Rameshkumar N. Arthrobacter pokkalii Sp Nov, a novel plant associated actinobacterium with plant beneficial properties, isolated from saline tolerant Pokkali rice, Kerala, India. PLoS ONE. 2016;11:e0150322.
92. Barnawal D, Bharti N, Maji D, Chanotiya CS, Kalra A. ACC deaminase-containing Arthrobacter protophormiae induces NaCl stress tolerance

through reduced ACC oxidase activity and ethylene production resulting in improved nodulation and mycorrhization in Pisum sativum. J Plant Physiol. 2014;171:884–94.
93. Xu L, Zhang H, Xing Y-T, Li N, Wang S, Sun J-Q. Complete genome sequence of Sphingobacterium psychroaquaticum strain SJ-25, an aerobic bacterium capable of suppressing fungal pathogens. Curr Microbiol. 2020;77:115–22.
94. Ahmed I, Ehsan M, Sin Y, Paek J, Khalid N, Hayat R, et al. Sphingobacterium Pakistanensis Sp. nov., a novel plant growth promoting rhizobacteria isolated from rhizosphere of Vigna mungo. Antonie Van Leeuwenhoek. 2014;105:325–33.
95. Mehnaz S, Weselowski B, Lazarovits G. Sphingobacterium canadense Sp. nov., an isolate from corn roots. Syst Appl Microbiol. 2007;30:519–24.
96. Akley EK, Rice CW, Adotey N, Ampim PAY, Vara Prasad PV, Owusu Danquah E, et al. Residual Bradyrhizobium inoculation effects on soybean performance and selected soil health parameters. Agron J. 2022;114:1627–41.
97. Meena RS, Vijayakumar V, Yadav GS, Mitran T. Response and interaction of Bradyrhizobium japonicum and arbuscular mycorrhizal fungi in the soybean rhizosphere. Plant Growth Regul. 2017;2017 842:84: 207–23.
98. Tarkka MT, Lehr NA, Hampp R, Schrey SD. Plant behavior upon contact with streptomycetes. Plant Signal Behav. 2008;3:917.
99. Duchateau S, Crouzet J, Dorey S, Aziz A. The plant-associated Pantoea spp. As biocontrol agents: mechanisms and diversity of bacteria-produced metabolites As a prospective tool for plant protection. Biol Control. 2024;188:105441.
100. Esmaeel Q, Miotto L, Rondeau M, Leclère V, Clément C, Jacquard C et al. Paraburkholderia phytofirmans PsJN-Plants interaction: from perception to the induced mechanisms. Front Microbiol. 2018;9:2093. https://doi.org/10.3389/fmicb.2018.02093.
101. Flores-Félix JD, Velázquez E, García-Fraile P, González-Andrés F, Silva LR, Rivas R. Rhizobium and Phyllobacterium bacterial inoculants increase bioactive compounds and quality of strawberries cultivated in field conditions. Food Res Int. 2018;111:416–22.
102. Darriaut R, Marzari T, Lailheugue V, Tran J, Martins G, Marguerit E et al. Microbial dysbiosis in roots and rhizosphere of grapevines experiencing decline is associated with active metabolic functions. Front Plant Sci. 2024;15:1358213. https://doi.org/10.3389/fpls.2024.1358213.
103. Ginnan NA, Dang T, Bodaghi S, Ruegger PM, McCollum G, England G, et al. Disease-induced microbial shifts in citrus indicate microbiome-derived responses to Huanglongbing across the disease severity spectrum. Phytobiomes J. 2020;4:375–87.
104. Vryzas Z. The plant as metaorganism and research on next-generation systemic pesticides - prospects and challenges. Front Microbiol. 2016;7:1968.
105. Kuiper I, Bloemberg GV, Noreen S, Thomas-Oates JE, Lugtenberg BJJ. Increased uptake of Putrescine in the rhizosphere inhibits competitive root colonization by Pseudomonas fluorescens strain WCS365. 2001;14(9):1096–104. https://doi.org/10.1094/MPMI.2001.14.9.1096.
106. Liu Z, Beskrovnaya P, Melnyk RA, Hossain SS, Khorasani S, O'sullivan LR, et al. A genome-wide screen identifies genes in rhizosphere-associated pseudomonas required to evade plant defenses. MBio. 2018;9:1–17.
107. Shi Z, Wang Q, Li Y, Liang Z, Xu L, Zhou J et al. Putrescine is an intraspecies and interkingdom cell-cell communication signal modulating the virulence of dickeya zeae. Front Microbiol. 2019;10:1950. https://doi.org/10.3389/fmicb.2019.01950.
108. Ramos-Ruiz R, Martinez F, Knauf-Beiter G. The effects of GABA in plants. Cogent Food Agric. 2019;5(1). https://doi.org/10.1080/23311932.2019.1670553.
109. Sun D. Pull in and push out: mechanisms of horizontal gene transfer in bacteria. Front Microbiol. 2018;9:2154.
110. Ghosh A, Passaris I, Mebrhatu MT, Rocha S, Vanoirbeek K, Hofkens J, et al. Cellular localization and dynamics of the Mrr type IV restriction endonuclease of *Escherichia coli*. Nucleic Acids Res. 2014;42:3908.
111. Ongena M, Jacques P. Bacillus lipopeptides: versatile weapons for plant disease biocontrol. Trends Microbiol. 2008;16:115–25.
112. Eschenbrenner M, Coves J, Fontecave M. The flavin reductase activity of the Flavoprotein component of sulfite reductase from Escherichia coli. A new model for the protein structure. J Biol Chem. 1995;270:20550–5.
113. Lewis RW, Islam A, Opdahl L, Davenport JR, Sullivan TS. Comparative genomics, siderophore production, and Iron scavenging potential of root zone soil Bacteria isolated from 'concord' grape vineyards. Microb Ecol. 2019;78:699–713.
114. Verbon EH, Trapet PL, Stringlis IA, Kruijs S, Bakker PAHM, Pieterse CMJ. Iron and immunity. Annu Rev Phytopathol. 2017;55:355–75.

Publisher's note